Bioresource Technology 169 (2014) 188–197

Contents lists available at ScienceDirect

Bioresource Technology

journal homepage: www.elsevier.com/locate/biortech

Catalytic pyrolysis of miscanthus × giganteus in a spouted bed reactor

Shoucheng Du, Yijia Sun, David P. Gamliel, Julia A. Valla, George M. Bollas *

Department of Chemical & Biomolecular Engineering, University of Connecticut, Storrs, 191 Auditorium Road, Unit 3222, Storrs, CT 06269-3222, USA

HIGHLIGHTS

- Design of a new conical spouted bed reactor for fast catalytic pyrolysis.
- Selectivity to aromatics increases with temperature and catalyst to biomass ratio.
- The ZSM-5 catalyst support promotes coke formation and reduces aromatics.
- Miscanthus catalyzed by ZSM-5 yields deoxygenated liquid products.

ARTICLE INFO

Article history:
Received 11 June 2014
Received in revised form 26 June 2014
Accepted 27 June 2014
Available online 5 July 2014

Keywords:
Biomass pyrolysis
Fast catalytic pyrolysis
Spouted bed reactor
ZSM-5 catalyst

ABSTRACT

A conical spouted bed reactor was designed and tested for fast catalytic pyrolysis of miscanthus × giganteus over Zeolite Socony Mobil-5 (ZSM-5) catalyst, in the temperature range of 400–600 °C and catalyst to biomass ratios 1:1–5:1. The effect of operating conditions on the lumped product distribution, bio-oil selectivity and gas composition was investigated. In particular, it was shown that higher temperature favors the production of gas and bio-oil aromatics and results in lower solid and liquid yields. Higher catalyst to biomass ratios increased the gas yield, at the expense of liquid and solid products, while enhancing aromatic selectivity. The separate catalytic effects of ZSM-5 catalyst and its Al_2O_3 support were studied. The support contributes to increased coke/char formation, due to the uncontrolled spatial distribution and activity of its alumina sites. The presence of ZSM-5 zeolite in the catalyst enhanced the production of aromatics due to its proper pore size distribution and activity.

© 2014 Elsevier Ltd. All rights reserved.

1. Introduction

Global energy unsustainability and environmental issues have generated interest in searching for alternative and renewable energy sources. Biomass has been a major source of energy for mankind dating back to ancient times. Today, it is the fourth largest source of energy in the world (Huber et al., 2006). Lignocellulosic biomass is the most abundant form of biomass, typically composed of cellulose (38–50%), hemicellulose (23–32%) and lignin (15–25%). Renewable woody biomass can be transformed into liquid, gaseous and solid fuels or fuel precursors through pyrolysis, thereby decreasing our dependency on fossil fuels. However, thermal pyrolysis of lignocellulosic biomass produces a bio-oil of low quality, due to its high oxygen content, high acidity, and low calorific value. Catalytic pyrolysis has been shown to be an effective way to enhance deoxygenation reactions, thus improving the bio-oil quality. Furthermore, fast heating rates also improve the bio-oil quality (Huber et al., 2006). Therefore, fast catalytic pyrolysis (or catalytic fast pyrolysis) was studied and shown to be among the most effective processes for the conversion of lignocellulosic biomass to fuels and chemicals.

Various reactor configurations have been used in fast catalytic pyrolysis studies. Micro-pyroprobe reactors have been widely applied in the study of fast catalytic pyrolysis of biomass due to their ease of operation (Foster et al., 2012; Patwardhan et al., 2011), but they entail intrinsic limitations such as inefficient biomass/catalyst mixing, small biomass loading and particle size. Moreover, they cannot be economically scaled up to satisfy industrial needs (Carlson et al., 2011); they are useful only for bench-scale studies. On the contrary, fluidized bed reactors have been extensively utilized in chemical processes across industry due to their scalability, excellent mass and heat transfer properties, good mixing between the solids and suspending fluid, uniform catalyst distribution, ability to operate continuously and so forth. Therefore, it is of industrial relevance to study biomass pyrolysis in fluidized bed reactors, focusing on more realistic bench-scale experimentation and simulation. One type of fluidized bed reactor is the spouted-bed design, which has been shown to be ideal for application to biomass pyrolysis. It can handle large particle size

* Corresponding author.
E-mail address: george.bollas@uconn.edu (G.M. Bollas).

http://dx.doi.org/10.1016/j.biortech.2014.06.104
0960-8524/© 2014 Elsevier Ltd. All rights reserved.

distributions, larger particles, differences in particle densities, and provides excellent mixing (Cui and Grace, 2008).

The effect of operating conditions, such as temperature and catalyst to biomass ratio, on biomass catalytic pyrolysis product distributions have been widely investigated in the literature. Zhang et al. (2012) studied the effect of temperature and weight hourly space velocity (WHSV) on product selectivity in pyrolysis of pine wood with ZSM-5 in a fluidized bed reactor. They showed that the maximum aromatic yield (13.9%, mainly benzene, toluene, xylene and naphthalene) was achieved at 600 °C and 0.35 h^{-1} WHSV (catalyst to biomass ratio of ~6). Thangalazhy-Gopakumar et al. (2012) performed catalytic pyrolysis of green algae in a pyroprobe and observed a 13.9% maximum aromatic yield at 650 °C and a catalyst to biomass ratio of 9. Bilbao and co-workers studied the spouting characteristics and the advantages of spouted beds, with specific applications to biomass pyrolysis (Olazar et al., 2000). However, other than their extensive work, a comprehensive study of the effect of operating conditions (temperature and catalyst to biomass ratio) on the product distribution in biomass catalytic pyrolysis in spouted bed reactors has not been published.

In this work, a bench-scale conical spouted-bed reactor was designed, using published correlations for the stability of the spouting regime and considering different particle properties, geometric factors and important hydrodynamic parameters. The challenges and advantages of the developed experimental setup are discussed and illustrated. With the specially designed reactor, fast catalytic pyrolysis of miscanthus giganteus was studied. The effects of temperature (400–600 °C) and catalyst to biomass ratio (1:1–5:1) on biomass fast catalytic pyrolysis product distribution and selectivity are investigated. In addition, the contribution of ZSM-5 catalyst support on the product distribution and selectivity is explored.

2. Experimental section

2.1. Feedstock and catalyst

Various lignocellulosic biomass sources have been investigated for bio-oil production through fast catalytic pyrolysis, including pine wood, rice straw and wheat straw. Among biomass feedstocks, miscanthus is a promising energy crop due to its simple cultivation, high calorific value and fast growth rate (Park et al., 2012). In this study, miscanthus is used as the biomass feedstock. The feed is grinded and dried in an oven at 120 °C overnight and then sieved to 80–175 μm particle size. Proximate analysis of the feedstock is performed in a Q-500 thermogravimetric analyzer from TA Instruments, following literature protocols (Cassel et al., 2012). Ultimate analysis of the feedstock is carried out in a Vario MicroCube elemental analyzer from Elementar. The results of proximate and ultimate analysis are shown in Table 1. Commercial ZSM-5 catalyst and Al_2O_3–SiO_2 matrix from W. R. Grace & Co. are used as the catalysts in this study. Table 2 shows basic information about the ZSM-5 catalyst and the Al_2O_3–SiO_2 matrix, including porosity and acidity. Comprehensive characterization of the ZSM-5 catalyst in terms of morphology and pore size distribution, and the deactivation of the catalyst due to coke and char formation during biomass (catalytic) pyrolysis were presented previously (Du et al., 2013a).

Table 1
Proximate and ultimate analysis of the miscanthus feedstock.

Proximate analysis (wt%)		Ultimate analysis (wt%)	
Moisture	4.81	C	40.94
Volatile	83.89	H	5.23
Fixed carbon	6.47	N	0.18
Ash	4.83	S	0.32
		O[a]	53.33

[a] Oxygen is calculated by difference.

2.2. Experimental setup and procedure

Fig. 1 illustrates the spouted bed reactor setup, which includes the conical spouted bed reactor housed inside an electrical furnace, biomass and catalyst feeders, liquid collection system and Fourier Transform Infrared Spectroscopy (FTIR) for on-line gas analysis. The dimensions of the spouted bed reactor are also shown in Fig. 1. The biomass is fed by the biomass auger feeder from the bottom of the reactor. The catalyst is fed *via* entrainment from the catalyst feeder also from the bottom of the reactor. The liquid collection system contains six impingers submerged in a dry ice bath. The FTIR is connected, on-line, downstream the liquid collection system and analyzes the gas composition as a function of time.

Considerable effort was devoted on designing the biomass feeding system. Dai et al. (2012) reviewed and discussed common biomass feeding problems, such as bridging and line blockages occurring in biomass thermochemical processes. The issues in biomass feeding were also studied by an international group of researchers (Nowakowski et al., 2010). For the extreme case of lignin pyrolysis, they showed that significant amounts of char can be accumulated on the auger, unless special cooling designs are applied. This obviously affects the accuracy and consistency of bench-scale experiments and could potentially impact the operational stability and economics of the corresponding commercial equivalents. The spouted bed unit of the group of Bilbao and coworkers (Olazar et al., 2000) has a hopper feeder system at the reactor top, which addresses the problems of auger feeding. However, depending on the setup and conditions, part of the biomass could be pyrolyzed at the top dilute zone and exit the reactor without being catalytically upgraded. Also, fine biomass particles might be entrained out of the reactor before conversion to gas or bio-oil. In order to address these challenges, namely char formation on the feeder, blockage of the transfer line, inefficient contacting with catalyst, and fine particle entrainment, our reactor was designed to accept biomass from the bottom via entrainment (Fig. 1). A cooling jacket was applied to keep the inlet of the reactor below 100 °C, thus eliminating blockage of the inlet caused by low temperature thermal pyrolysis of biomass. Thus, with the current design, biomass does not react until it contacts the hot catalyst bed inside the reactor.

In all the experiments, the catalyst was loaded into the reactor *via* entrainment. When the desired pyrolysis temperature was achieved (measured with a thermocouple inside the catalyst bed), biomass was fed at a rate of 4 gr/min for 1 min, using an auger feeder and a vertical entrainment line with 5 SL/min N_2 flow. During the reaction, volatile matter, which includes organic vapors and permanent gas, exits the top of the reactor and passes through a condensing system. The organic vapors are condensed in a six-impinger train in a dry-ice bath. Methanol was used as a solvent to trap the organic vapors. The intermediate line between the reactor outlet and the impinger train was maintained at 300 °C, to prevent condensation of organic vapors in the line. The total time for reaction and purging was 10 min for all the experiments. After the experiment, the reactor was cooled down and washed with water. The water/char/catalyst mixture was dried overnight and then analyzed. The impingers were washed with methanol and the entrained solid particles were filtered out using a vacuum pump. The lumped char/coke yield is presented as the sum of the entrained solid particles and the solids obtained from the water/char/catalyst mixture subtracting the original catalyst load. All the experiments presented here are repeated at least three times

Table 2
Characterization of the supported ZSM-5 catalyst and Al_2O_3–SiO_2 matrix[a].

	Physical property		Porosity analysis[b]			Acidity analysis[c]		
	ρ_{bulk} (kg/m^3)	d_p (μm)	S_{total} (m^2/g)	S_{micro} (m^2/g)	V_{micro} (cm^3/g)	B.s. (μmol/g)	L.s. (μmol/g)	B.s./L.s
ZSM-5	800	75∼175	124.30	98.98	4.61E-2	35.26	3.16	11.15
Matrix	860	70∼230	157.79	4.29	2.11E-4	2.07	35.36	0.06

[a] In Table 2, ρ_{bulk} stands for bulk density; d_p, particle size; S_{total}, BET surface area; S_{micro}, *t*-plot micropore area; V_{micro}, *t*-plot micropore volume; B.s., Brønsted acid sites; L.s., Lewis acid sites.
[b] Porosity analysis was performed in Micromeritics ASAP 2020 Accelerated Surface Area and Porosimetry System. Samples were degassed at 250 °C under vacuum for 12 h before analysis.
[c] Acidity analysis was performed by Diffuse Reflectance Infrared Fourier Transform Spectroscopy (DRIFTS). ZSM-5 and matrix were calcined in air at 350 °C for 3 h, and then diluted with KBr to 6 wt%. Enough pyridine (99 wt%) was added to the samples to achieve saturation. Physisorbed pyridine was removed by heating the samples to 150 °C under vacuum. Extinction coefficients of 1.67 cm/μmol and 2.22 cm/μmol are used for concentration calculation of Brønsted and Lewis acid sites, respectively (Iliopoulou et al., 2012).

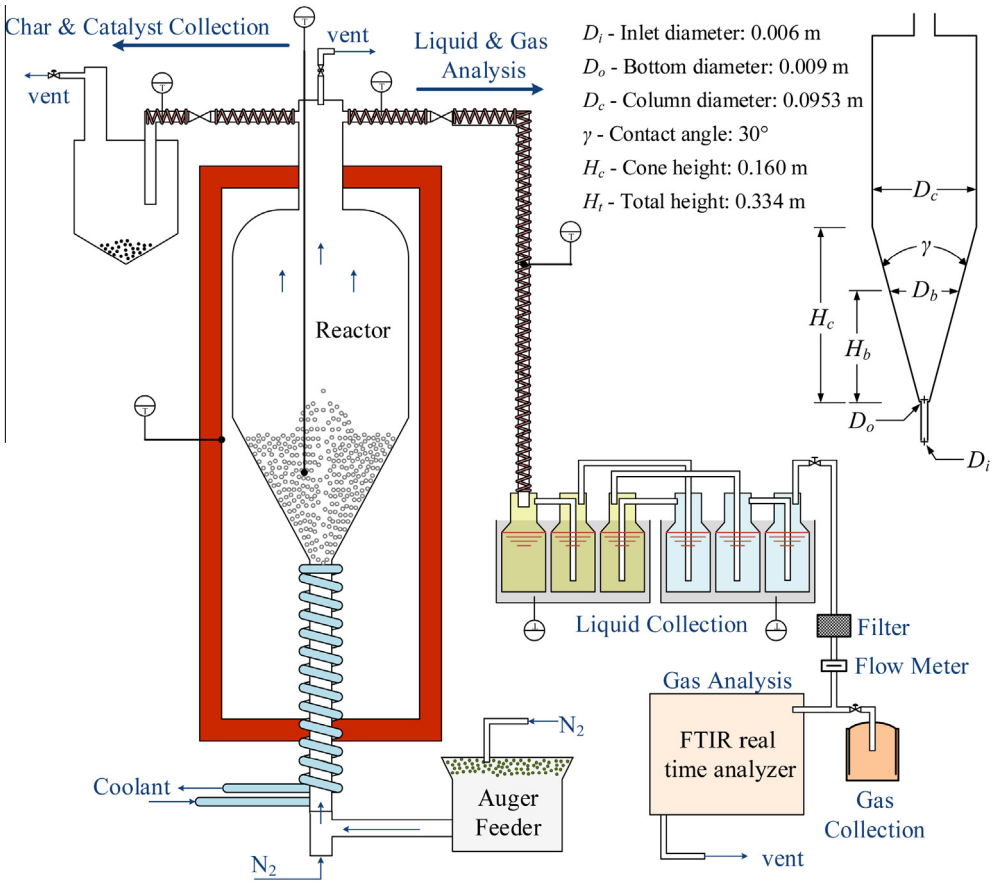

Fig. 1. Conical spouted bed reactor setup for biomass catalytic pyrolysis.

or as many required for the overall mass balance of each experiment to be >90%.

2.3. Bio-oil and gas analysis

The bio-oil, condensed in the impinger train, was washed with methanol and collected. The total volume of the diluted bio-oil was then measured. The diluted bio-oil was analyzed in an Agilent 6890 N Gas Chromatograph (GC) (Agilent DB-5 column) equipped with a 5973 N mass selective detector (MS). The GC oven was held initially at 40 °C for 2 min and then ramped to 270 °C at 10 °C/min. Quantification was performed with benzene, toluene, xylene, ethylbenzene, styrene, benzofuran, indane, naphthalene, naphthalene, 1-methyl naphthalene, biphenyl, diphenylmethane, acenaphthalene, fluorene, phenanthrene and anthracene external standards, and the method of semi-quantification was applied for the remainder of the identified compounds. In this study, the liquid products are measured and reported in two ways: the lumped yield (including water) obtained by measuring the weight of impingers before and after pyrolysis (excluding the weight of entrained solids), and the bio-oil distribution measured by GC–MS.

Gas composition analysis was performed using a Thermo Nicolet 6700 FTIR with a 2-meter gas cell. A scan number of 16 was used with a resolution of 1 cm^{-1} and optical velocity of 6.3290 cm/s. The collection of each data point took 11 s, allowing for real-time gas analysis. The total mole fraction for each gas component is calculated by integrating its spectrum area over the time of experiment. Due to the low content of sulfur in the miscanthus

used (Table 1) and the broader focus of this study, the sulfur products were not analyzed and the reactions between zeolite and sulfur are not considered or reported.

3. Results and discussion

3.1. Design of the spouted bed reactor and hydrodynamic analysis

Table 3 shows the dimensions of the spouted bed reactor and the respective measurements of the pressure drop and minimum spouting flow rate. For the design of the spouted bed reactor, the minimum spouting flow rate and the maximum pressure drop were first calculated based on correlations discussed in the Supplementary Information. According to this hydrodynamic analysis for all the experimental conditions, a 5 SL/min flow rate was found sufficient for stable spouting. This was validated with cold- and hot- flow experiments in a fused quartz tube reactor. As shown in the Supplementary Information, the measurements of minimum spouting velocity and pressure drop are in reasonable agreement with the literature correlations used for designing the reactor. Thereafter, a comprehensive analysis was performed to identify the stable hydrodynamic regimes, in which the designed reactor fell in. According to Fig. S1, the operating regimes studied were well within the acceptable ranges for stable fluidization in conical spouted beds.

3.2. Overview of the effect of operating conditions on product distribution

Fig. 2(a–c) illustrates the overall effect of temperature (400–600 °C) and catalyst to biomass ratio (1–5) on the product distribution, lumped as total liquid, gas and solid. Generally, at higher temperatures, more gas products and less liquid and solid products were obtained. The catalytic effect was enhanced at higher temperature, thus more CO and CO_2 were produced through deoxygenation reactions. At higher catalyst to biomass ratio, higher gas yield and lower liquid and solid yields were observed, due to enhanced catalytic reactions. A detailed discussion on the effect of temperature and catalyst to biomass ratio on the lumped product distribution, bio-oil selectivity and gas composition is presented in the following sections. We note that in all the experiments performed in this study, a clear linear relationship between aromatic yield and CO yield could be observed, shown in Fig. 2(d). This is discussed further in Section 3.8. This served as a validation of the consistency of the effectiveness of the catalytic effect in the spouted bed reactor within the temperature range studied, showing that catalytic deoxygenation results in better aromatic selectivity.

As mentioned in the experimental section, all experiments were repeated at least three times and those with mass balance <90% were discarded. In Fig. 2(a–c), standard deviations are shown for each trial in order to show the accuracy and consistency of each experiment. To be specific, at 400 °C, the maximum standard deviation was 2.21% for the liquid product, 2.12% for the solid product and 2.13% for the gas product. The respective values at 500 °C were 2.19% for the liquid product, 1.97% for the solid product; 2.11% for the gas product. At 600 °C, the values were 1.09% for the liquid product, 2.21% for the solid product, and 2.55% for the gas product. The overall mass balance for all the experiments was higher than 90%, within the range of 92.23–104.51%.

3.3. Effect of temperature on the lumped product distribution

Fig. 3(a) shows the effect of temperature on the lumped product distribution. As the temperature increased from 400 °C to 600 °C, the gas yield increased significantly from ~16 wt% to ~25 wt%, whereas the solid and liquid yields decreased from ~43 wt% to ~35 wt% and from ~43 wt% to ~33 wt%, respectively. A similar effect of temperature on the product distribution was observed by Williams and Nugranad (2000), who studied catalytic pyrolysis of rice husks with ZSM-5 catalyst in a fluidized bed reactor. They found that as temperature increased, the liquid and solid yields decreased in parallel to higher gas production. The increase in gas yield at higher temperature was mostly because of the production of carbon monoxide (see Section 3.5), which was caused by decomposition of the solid fraction and secondary reactions of the liquid fraction to volatile compounds in the reactor at higher temperature (Pütün et al., 2006). The overall mass balance for each experiment is also shown in Fig. 3(a) with the error bars. The error bars shown in Fig. 3(a) represent the variation of each lumped yield measured over three successful trials. The total yields measured (mass balance) were 102.02%, 97.69% and 93.38% for temperatures of 400 °C, 500 °C, and 600 °C, respectively. The standard deviations for the total yields were within the range of 0.415–3.76% for all the experiments studied at different temperatures.

3.4. Effect of temperature on bio-oil distribution

Fig. 3(c) illustrates the effect of temperature on the bio-oil distribution at a catalyst to biomass ratio of 1. The total aromatic yield increased with temperature (400–600 °C), from 3.25 wt% to 5.96 wt%. In particular, at 400 °C, no monocyclic aromatic hydrocarbons (benzene, toluene, xylene, styrene, and alkylbenzenes) were observed in the bio-oil. As temperature was increased, the yield to monocyclic aromatic hydrocarbons increased. The increase in monocyclic hydrocarbons with temperature could be explained by the promotion of decomposition reactions at higher temperature, producing smaller compounds, which had easier access to the ZSM-5 zeolite pores (Wang et al., 2014). The yield to indenes, naphthalenes and heavier polycyclic aromatic hydrocarbons (PAHs) also increased with temperature. The formation of polyaromatic compounds was attributed by Aho et al. (2007) to the Brønsted acidity of zeolite in the catalyst, which promoted acid catalyzed reactions, such as cracking, dimerization, cyclization and dehydrocyclization. The yield to phenols, benzofurans, and other oxygenates (mainly acetic acid) decreased as the

Table 3
Experimental conditions and hydrodynamic measurements[a].

Temperature (°C)	400/500/600	400/500/600	400/500/600
Catalyst/biomass ratio	1:1	2:1	5:1
Catalyst inventory, W_C (gr)	4	8	20
Stagnant bed height, H_b (m)	0.025	0.035	0.053
Stagnant bed top diameter, D_b (m)	0.022	0.028	0.037
Observed pressure drop ΔP_{exp} (atm)	0.002	0.004	0.007
Observed min. spouting at 25 °C	3.25	4.57	10.5

[a] All the experiments are batch, performed with N_2 flow of 5 SL/min for 10 min.

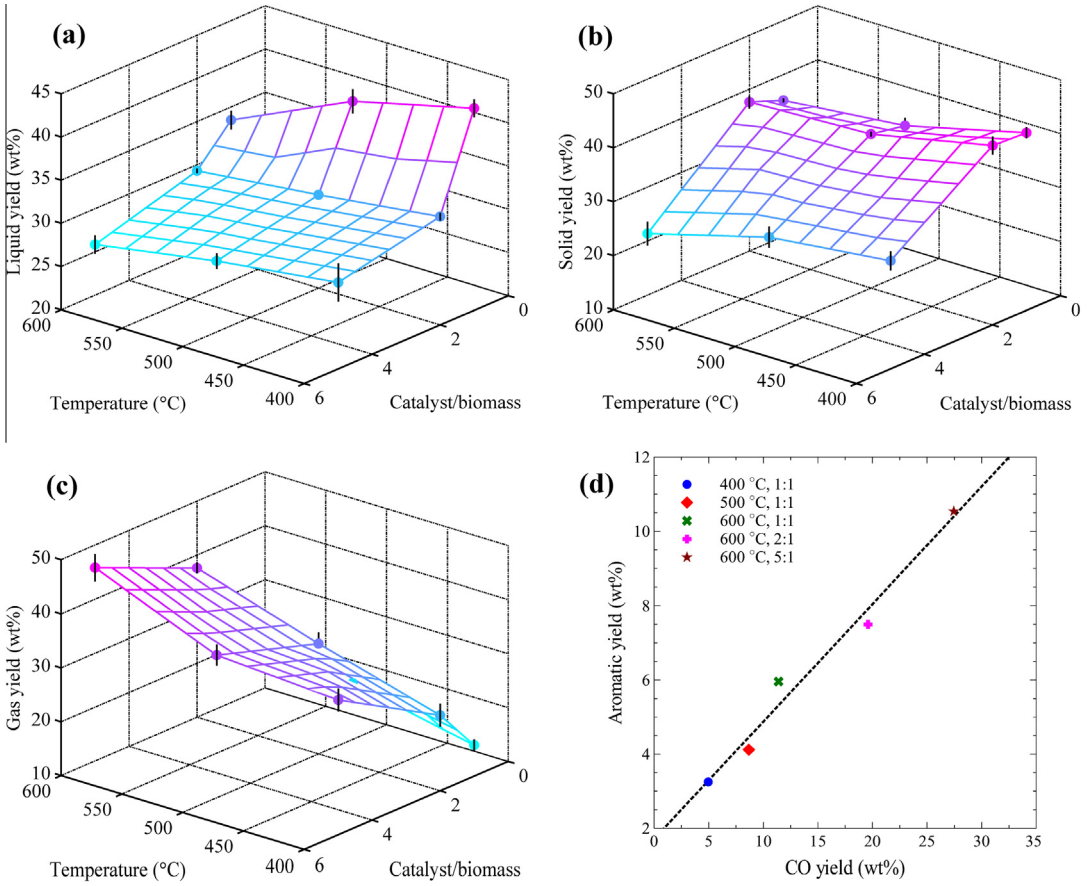

Fig. 2. Effect of operating conditions on (a–c) the lumped product distribution; and (d) the relationship between aromatics and CO yields. Liquid product includes water and organic compounds. Solid product includes char and coke.

temperature increased. This reflects that higher temperatures enhance deoxygenation reactions, which was also evidenced by the higher yields to CO and CO_2.

3.5. Effect of temperature on gas yield

Five major gaseous compounds, CO, CO_2, CH_4, C_2H_2, and C_2H_4 were quantified on-line with FTIR. As shown in Fig. 3(b), when the temperature increased, the yields to all gas products increased. CO was the most abundant component in the vapor products and increased significantly from 4.95 wt% to 11.39 wt%, with a temperature increase from 400 °C to 600 °C. The yield to CO_2 and CH_4 did not change much with temperature. The yield to olefins increased from 5.26 wt% at 400 °C to 7 wt% at 600 °C. The CO/CO_2 weight ratio changed from 1.49 to 2.86 when the temperature increased from 400 °C to 600 °C. This is comparable with Zhang et al. (2012), who measured 1.45–2.42 CO/CO_2 weight ratios at temperatures between 400–650 °C. Similar results were also obtained by Wang et al. (2014), who studied catalytic pyrolysis of individual components of lignocellulosic biomass (cellulose, hemicellulose and lignin) at 600 °C. They reported 2.19, 1.56 and 2.07 CO/CO_2 ratios for the catalytic pyrolysis of cellulose, hemicellulose and lignin, respectively. However, not all the relevant analyses of CO/CO_2 ratio were consistent. Olazar et al. (2000) reported a CO/CO_2 ratio of 0.08–0.22 for the catalytic pyrolysis of pine sawdust with ZSM-5 catalyst over a temperature range of 400–500 °C. Williams and Nugranad (2000) observed CO/CO_2 ratios close to unity after pyrolysis of rice husks with ZSM-5 catalyst at temperatures between 400–600 °C. On the contrary, Wang et al. (2014) claimed that the strong acid sites of their H-ZSM-5 catalyst were more active for decarbonylation to produce CO than decarboxylation to CO_2. Evidently, differences in the acidity of the various ZSM-5 catalysts used in each experimental work and differences in feedstock composition make the comparison of gas selectivity difficult.

3.6. Effect of catalyst to biomass ratio (C/B) and weight hourly space velocity (WHSV) on the lumped product distribution

In this study, catalyst to biomass ratio was varied by changing the catalyst loading and maintaining the biomass feed rate and total amount fed. Thus, C/B ratio and WHSV were not controlled independently. Therefore, the effect of catalyst to biomass ratio on product distribution, shown in Fig. 4(a), was actually the combined effect of C/B ratio and WHSV. As shown in Fig. 4(a), the gas yield increased with increasing catalyst to biomass ratio, whereas the solid and liquid yields decreased. The overall mass balance for each experiment is also shown in Fig. 4(a) with error bars. The errors shown here also represent the variation of each yield measured over the three successful trials. The total yields measured (mass balance) were 93.38%, 104.51% and 93.00% for temperatures of 400 °C, 500 °C, and 600 °C, respectively. The standard deviations for the total yields were within the range of 0.635–7.24% for all the experiments studied by changing the C/B ratio.

Fig. 5 shows a review of the effect of catalyst to biomass ratio and WHSV on the lumped product distribution. Atutxa et al. (2005) studied the catalytic pyrolysis of pine sawdust with ZSM-5 catalyst in a spouted bed reactor at 400 °C. They changed the catalyst to biomass ratio at constant bed height but different catalyst loadings (supplementing the difference with silica sand). They found that as the catalyst to biomass ratio increased the gas yield

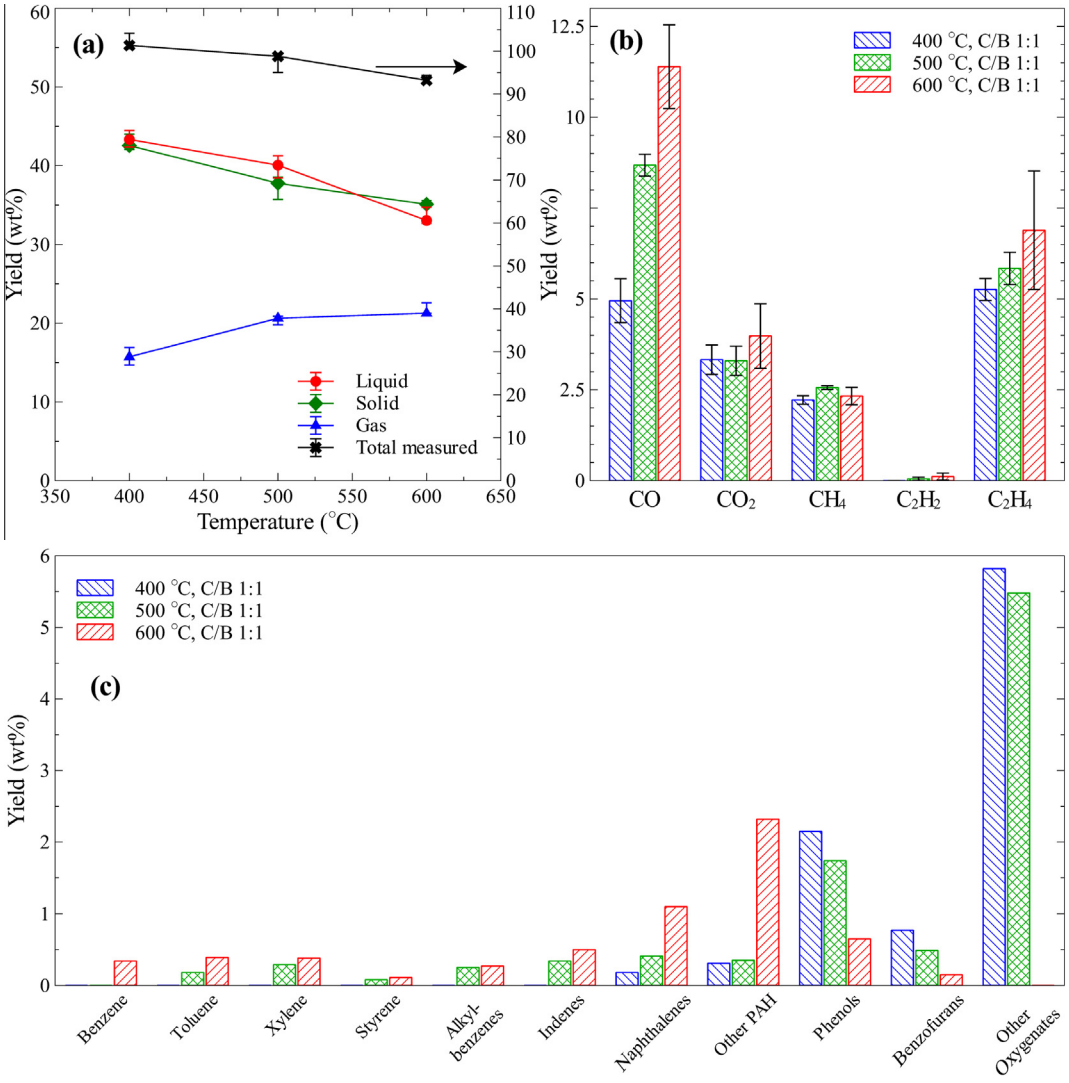

Fig. 3. Effect of temperature on (a) the lumped product distribution; (b) the gas product distribution and (c) the bio-oil distribution. Liquid product includes water and organic compounds. Solid product includes char and coke. Alkylbenzenes mainly include benzene, 1-ethyl-2-methyl-, benzene, 1-butynyl-, benzene, 1,2,3,5-tetramethyl-, benzene, ethenylmethyl-, benzene, cyclopropyl-. Indenes mainly include indene, indane, 2-methylindene, 1H-indene, 1,3-dimethyl-. Naphthalenes mainly include naphthalene, naphthalene, 1,2-dihydro-, naphthalene, 2-methyl-, naphthalene, 1-methyl-, naphthalene, 2-ethenyl, naphthalene, 2-ethyl-, naphthalene, 2,7-dimethyl-. Other PAH mainly include phenanthrene, anthracene, fluoranthene, pyrene, and their derivatives. Phenols mainly include phenol, phenol, 3-methyl-, phenol, 2-methoxy-, phenol, 2-methoxy-4-methyl-, phenol, 2,6-dimethoxy-4-(2-propenyl)-, phenol, 2,3-dimethyl-, phenol, 4-ethyl-, vanillin, eugenol. Benzofurans mainly include benzofuran, furfural, benzofuran, 2-methyl-, benzofuran, 2,3-dihydro-, benzofuran, 7-methyl-. Other oxygenates mainly include acetic acid, 1,2-cyclopentanedione, 2-cyclopenten-1-one, 2-hydroxy-3-methyl-, 2-cyclopenten-1-one, 2-methyl-.

increased, whereas the solid yield and the liquid yields decreased. Naqvi et al. (2014) studied catalytic pyrolysis of paddy husk in a fixed bed reactor with ZSM-5 catalyst. In their setup, C/B ratio and WHSV were not controlled independently. They found that liquid and solid yields decreased with increasing catalyst to biomass ratio (0.5–2), whereas the gas yield increased with the addition of catalyst due to catalyst promoted decarbonylation and decarboxylation reactions. Similar trends were also obtained by Wang et al. (2012), who studied catalytic pyrolysis of Douglas fir pellets in microwave with ZSM-5 catalyst, changing C/B ratio and WHSV simultaneously. Lappas et al. (2002), in catalytic pyrolysis experiments of lignocellulose in a circulating fluidized bed reactor with ZSM-5 catalyst, studied the effect of C/B ratio at constant WHSV. Although they observed similar trends for the yield to liquid and gas with the change in C/B ratio, the yield to solid was reported to be increasing with the catalyst to biomass ratio. An increase in the coke yield with catalyst loading was also observed by Jae et al. (2014), who studied the effect of C/B ratio at constant WHSV in catalytic pyrolysis of wood over ZSM-5 catalyst in a bubbling fluidized bed reactor.

In summary, the effect of catalyst to biomass ratio on liquid and gas distributions is generally consistent between the current study and the literature. The increase of catalyst to biomass ratio typically results in a decrease of the liquid yield, which is converted to gas products. This indicates the effect of the catalyst in promoting deoxygenation reactions, since oxygen removal from the bio-oil proceeds mostly via production of carbon oxides at relatively high temperature (>450 °C) (Naqvi et al., 2014). The inconsistency in the literature in the coke selectivity as a function of the catalyst to biomass ratio might be attributed to a combined effect of catalyst to biomass ratio and WHSV. Specifically, by changing catalyst to biomass ratio only, as was done by Lappas et al. (2002) and Jae et al. (2014), higher C/B ratios lead to higher coke yields. However, when the catalyst to biomass ratio and WHSV are changed simultaneously, such as in this study, Naqvi et al. (2014) and Wang et al. (2012), the coke yield decreases with higher catalyst to biomass

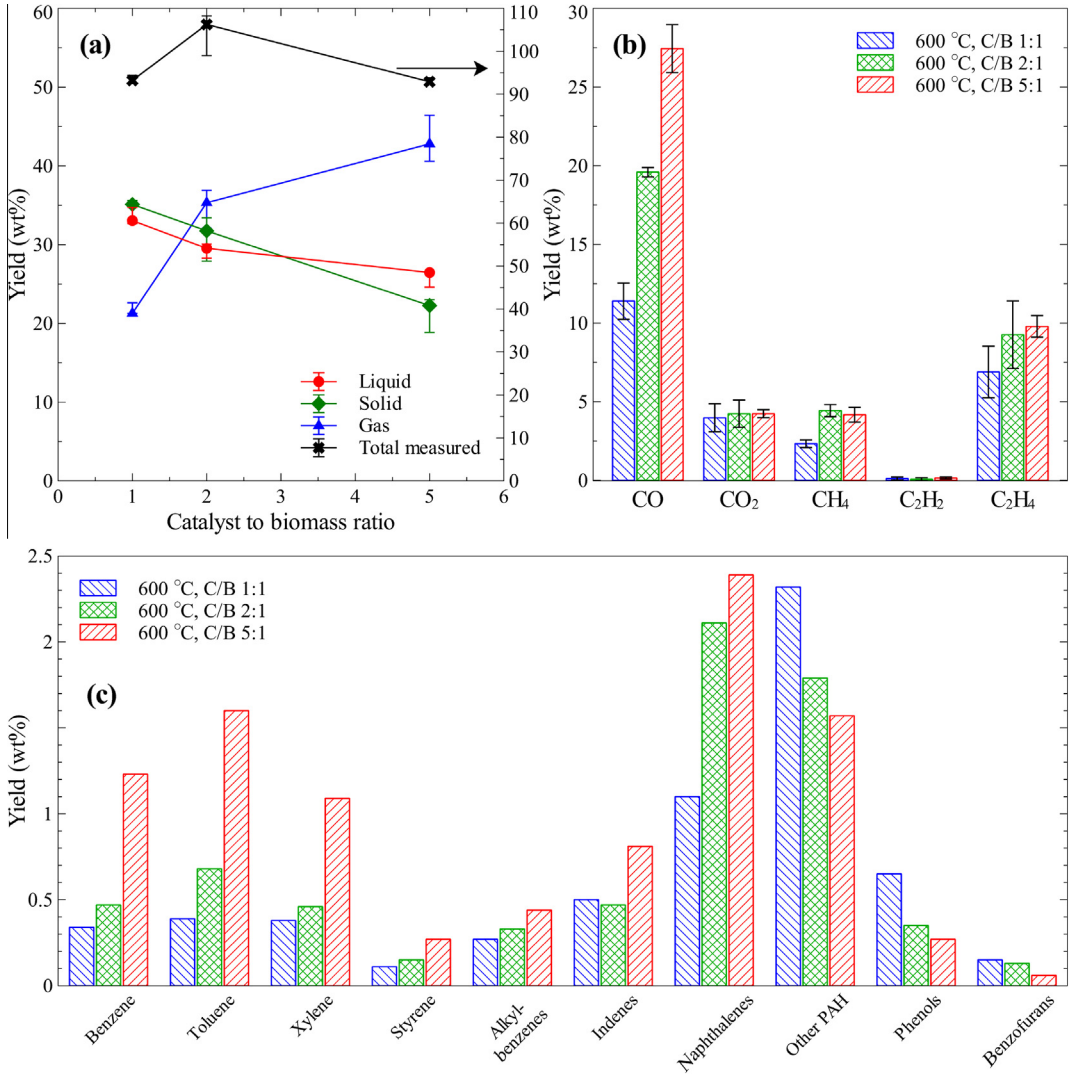

Fig. 4. Effect of catalyst to biomass ratio on (a) the lumped product distribution; (b) the gas product distribution and (c) the bio-oil distribution. Compound notation is as shown in Fig. 3.

ratio, due to the correspondingly decreasing WHSVs, higher residence times and bed heights (Patwardhan et al., 2011). As discussed previously (Du et al., 2013a), the solid pyrolysis product is a mixture of coke and char. Coke as a catalytic product should depend on the catalyst to biomass ratio; whereas, char as a thermal product should depend on residence time and bed height. Since char and coke have different origins in the cellulose, hemicellulose and lignin components of biomass (Du et al., 2013a), it is fairly difficult to obtain consistency in the observations between researchers using different reactor setups, feedstocks and catalysts.

3.7. Effect of catalyst to biomass ratio on bio-oil distribution

Fig. 4(c) shows the effect of catalyst to biomass ratio on bio-oil composition. The total aromatic yield increased from 5.96 wt% at a ratio of 1:1 to 10.54 wt% at a ratio 5:1. The observed increase in aromatics in the liquid was in good agreement with the literature. A brief summary of the aromatic selectivity in biomass catalytic pyrolysis in the literature is shown in Table 4. Despite the differences between the setups, feedstock, and operating conditions, the total aromatic yield (wt%) obtained from catalytic pyrolysis with ZSM-5 was measured in the range of 0.58–12.9 wt%. In the current study, the selectivity of monocyclic aromatic hydrocarbons (MAH), benzene, toluene, xylene, styrene and alkylbenzenes, was significantly promoted as the catalyst to biomass ratio increased. The total yield to PAHs also increased at higher catalyst to biomass ratios. Formation of PAHs was shown to be enhanced by catalytic reactions during pyrolysis (Williams and Nugranad, 2000). In particular, indenes and naphthalenes yields increased with catalyst to biomass ratio, whereas heavier PAHs, such as anthracenes, phenanthrenes and pyrenes, decreased with catalyst to biomass ratio. The yield to phenolic compounds decreased at higher catalyst loadings, illustrating the enhancement of deoxygenation reactions. As discussed in Section 3.4 and shown in Fig. 3(c), the yield of MAH reached the maximum 5.96 wt% at 600 °C, resulting in an optimum pyrolysis temperature of 600 °C. Additionally, the maximum in MAH selectivity, 10.54 wt%, was achieved at a catalyst to biomass ratio of 5:1, as shown in Fig. 4(c).

3.8. Effect of catalyst to biomass ratio on gas composition

Fig. 4(b) shows the effect of catalyst to biomass ratio on the gas distribution. As the catalyst to biomass ratio increased (1:1–5:1), the total gas yield increased from 24.70 wt% to 45.79 wt%. The selectivity of CO increased from ~46 wt% to ~60 wt% and the CO/CO_2 weight ratio increased from 2.86 to 6.47 with the increase in

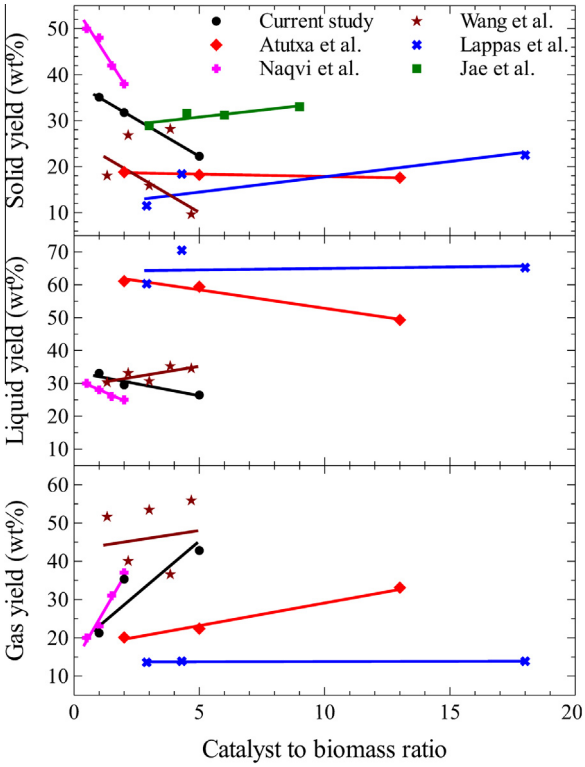

Fig. 5. Summary of the effect of catalyst to biomass ratio on the lumped product distribution from the current study and the literature. All the reported yields here are in wt%. Solid yields in C% from Jae et al. (Jae et al., 2014) were assumed to equal the solid yields in wt% feed basis.

catalyst to biomass ratio. Olefin yields also increased with catalyst to biomass ratio, from 7.00 wt% to 9.93 wt%. Combining the experiments of varying catalyst to biomass ratios with those of varying temperature, a clear linear relationship between aromatic yield and CO yield could be observed, as shown in Fig. 2(d). Foster et al. (2012) studied catalytic pyrolysis of glucose over ZSM-5 catalysts with varying SiO_2/Al_2O_3 composition. They suggested a possible correlation between CO production via decarbonylation and the formation of aromatics. Also, Wang et al. (2014) studied catalytic pyrolysis of cellulose, hemicellulose, and lignin at 600 °C with a catalyst to biomass ratio of 20. They showed a linear correlation between the aromatic yield and catalytic CO yield, from experiments with the three individual biomass components under the same conditions. This showed that the formation of aromatics was from the catalytic reactions of volatile intermediates, which were produced mainly through decarbonylation pathways.

3.9. Effect of presence of ZSM-5 on product distribution and bio-oil selectivity

To further understand the effect of ZSM-5 catalyst, experiments with pure catalyst support (matrix) were performed. Fig. 6(a) shows the product distribution from catalytic pyrolysis experiments with ZSM-5 catalyst and experiments with its matrix at different temperatures. It was clear that at each temperature, experiments with the matrix produced more char/coke than those with the ZSM-5 catalyst. The results are consistent with Stefanidis et al. (2011), who performed a catalyst screening study for upgrading of biomass pyrolysis vapors. They compared alumina (surface area 160 m^2/g) with the supported ZSM-5 catalyst (surface area 138 m^2/g) and showed that alumina produces more solids than ZSM-5 catalyst during the upgrading process. This indicates that

Table 4
Selectivity to aromatics and organic liquid in biomass catalytic pyrolysis from literature.

References	Reactor	Biomass	Catalyst	C/B ratio	Temp. (°C)	Aromatic yield (C%)	Aromatic yield (wt%)	Organic yield (wt%)[b]	Water yield (wt%)
(Foster et al. (2012))	Pyroprobe	Maple	ZSM-5	19	600	~26	~13[a]	~13	–
(Wang and Brown (2013))	Pyroprobe	Microalgae	ZSM-5	20	700	22.95	11.48[a]	11.48	–
(Thangalazhy-Gopakumar et al. (2012))	Pyroprobe	Algae	ZSM-5	1–9	650	2.6–25.8	1.3–12.9[a]	1.3–12.9	–
(Du et al. (2013b))	Pyroprobe	Microalgae	ZSM-5	1–5	550	–	6–17	6–17	–
(Srinivasan et al. (2012))	Pyroprobe	Pine	ZSM-5	9	450	14.88	7.44[a]	7.44	–
(Cheng et al. (2012))	Pyroprobe	Pine	ZSM-5	6	600	11.5	5.75[a]	5.75	–
(Zheng et al. (2014))	Pyroprobe	Pine	ZSM-5	9	600	18.9–23.4	9.45–11.7[a]	9.45–11.7	–
(Park et al. (2012))	Fixed bed	Miscanthus	ZSM-5	0.1	450	–	3.15	21.5	26.3
(Carlson et al. (2011))	Fluidized bed	Pine	ZSM-5	1.2–20	600	9.5–14	4.75–7[a]	4.75–7	–
(Zhang et al. (2012))	Fluidized bed	Pine	ZSM-5	1–5–18	600	4.4–13.9–6.7	2.2–6.95–3.35[a]	2.2–6.95–3.35	–
(Lappas et al. (2002))	Fluidized bed	Lignocell HBS	ZSM-5	2.9–18	400	–	0.58–0.64	36.4–30.7	23.9–34.5
(Zhang et al. (2009))	Fluidized bed	Corncob	ZSM-5	5	550	–	10.17	13.7	25.6
(Aho et al. (2008))	Fluidized bed	Pine	ZSM-5	0.4	450	–	8.5	20.7	13.0
(Mante et al. (2014))	Fluidized bed	Hybrid poplar	ZSM-5	0.5	500	~10.8	~5.4[a]	~27	~25
(Jae et al. (2014))	Fluidized bed	Pine	ZSM-5	3–9	600	11.9–13.9	5.95–6.95[a]	5.95–6.95	–
(Elordi et al. (2011))	Spouted bed	Polyethylene	ZSM-5	0.03	500	–	10	25	–
This work	Spouted bed	Miscanthus	ZSM-5	1–5	600	–	5.96–10.54	5.96–10.54	–

[a] Aromatic yield (wt%) is the standard yield out of biomass feedstock. Calculation has been performed to approximately convert carbon yield to standard yield by standard yield = 1/2 carbon yield.
[b] Organic yield includes the aromatics and other organic compounds, such as ketones, alcohols, aldehydes, acids.

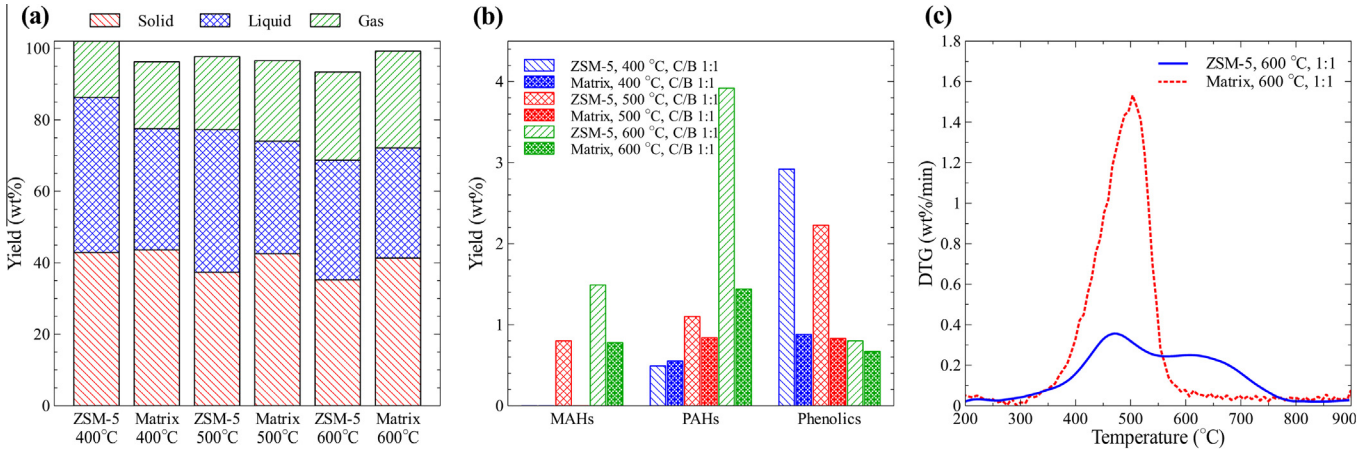

Fig. 6. Effect of ZSM-5 on (a) the lumped product distribution; (b) the bio-oil distribution; and (c) the solid product TPO. All six experiments are performed with catalyst to biomass ratio 1:1. TPO shown is of the coked ZSM-5 catalyst and catalyst matrix after catalytic pyrolysis at 600 °C and catalyst to biomass 1:1. MAHs mainly include benzene, toluene, xylene, styrene and alkylbenzenes. PAHs mainly include indenes, naphthalenes, and other PAHs such as phenanthrene, anthracene, fluoranthene, pyrene, and their derivatives. Phenolics mainly include phenols and benzofurans.

the matrix alone has activity due to the presence of alumina sites, which enhances non-selective pyrolysis reactions, forming coke/char. Coke and char form on both the support and the supported ZSM-5 catalyst, however the location of coke and char build-up is unclear in the literature. This study indicates that coke/char formation is highly promoted by the matrix, rather than the ZSM-5 catalyst. Fig. 6(c) shows the temperature programmed oxidation (TPO) in a thermogravimetric analyzer (TGA) of the coked ZSM-5 catalyst and the matrix (samples collected by washing the reactor and drying) from experiments at 600 °C and C/B ratio of 1. ZSM-5 coke/char TPO showed a low temperature peak and a high temperature peak, which represent char (higher oxygen content in the form of carbonyl groups formed on the matrix) (Du et al., 2013a) and coke (polyaromatic hydrocarbons mainly deposited in the micropores or cavities of ZSM-5), respectively. In comparison, TPO of the coked/charred matrix showed one peak at the same low temperature, identified as char for the ZSM-5 catalyst, but there was no high temperature peak. This indicated the absence of catalytic reactions, inside the catalyst pores and cavities, which lead to formation of polyaromatic coke (Du et al., 2013a) in the ZSM-5 catalyst.

Although the Al_2O_3-based matrix has activity, it did not improve the quality of the bio-oil, or enhance the selectivity to desired MAH compounds. As shown in Fig. 6(b), at low temperatures (400 °C and 500 °C), the matrix did not produce any MAH compounds. At 600 °C, low production of MAHs was observed with the matrix, but was significantly lower than that with the ZSM-5 catalyst. Also, the production of MAHs initially occurred at lower temperature (500 °C) with the ZSM-5 catalyst. In the temperature range studied, ZSM-5 produced more aromatics (including MAHs, PAHs, and Phenolics) than the matrix alone, due to the appropriate pore size and acidity of the ZSM-5 (Yu et al., 2012). The results verify that production of aromatics is favored by the presence of ZSM-5 catalyst.

4. Conclusions

The proposed spouted bed design was shown to be a promising reaction system for biomass fast catalytic pyrolysis of miscanthus, providing excellent mixing, superior biomass feeding and selectivity towards deoxygenated products. In agreement with relevant literature reports, high temperatures and catalyst loadings favor aromatic production, via deoxygenation reactions that form carbon oxides. The catalyst support produces more coke and less monocyclic aromatic hydrocarbons than the ZSM-5 catalyst, due to its uncontrolled catalytic activity and lack of shape selectivity. The product selectivity under different operating conditions was mapped, showing higher selectivity to aromatics at 600 °C and high catalyst to biomass ratios.

Acknowledgements

This material is based upon work supported by the National Science Foundation under Grant No. 1236738. The authors also thank W. R. Grace & Co. for supplying the catalysts used in this work and New Energy Farms Ltd. for providing the miscanthus feedstock for the experiments.

Appendix A. Supplementary data

Supplementary data associated with this article can be found, in the online version, at http://dx.doi.org/10.1016/j.biortech.2014.06.104.

References

Aho, A., Kumar, N., Eränen, K., Salmi, T., Hupa, M., Murzin, D.Y., 2008. Catalytic pyrolysis of woody biomass in a fluidized bed reactor: influence of the zeolite structure. Fuel 87, 2493–2501.

Aho, A., Kumar, N., Eränen, K., Salmi, T., Hupa, M., Murzin, D.Y., 2007. Catalytic pyrolysis of biomass in a fluidized bed reactor: influence of the acidity of H-Beta zeolite. Process Saf. Environ. Prot. 85, 473–480.

Atutxa, A., Aguado, R., Gayubo, A.G., Olazar, M., Bilbao, J., 2005. Kinetic description of the catalytic pyrolysis of biomass in a conical spouted bed reactor. Energy Fuels 19, 765–774.

Carlson, T.R., Cheng, Y.-T., Jae, J., Huber, G.W., 2011. Production of green aromatics and olefins by catalytic fast pyrolysis of wood sawdust. Energy Environ. Sci. 4, 145–161.

Cassel, B., Menard, K., Earnest, C., 2012. Proximate Analysis of Coal and Coke using the STA 8000 Simultaneous Thermal Analyzer. PerkinElmer, Inc. 1–4.

Cheng, Y.-T., Jae, J., Shi, J., Fan, W., Huber, G.W., 2012. Production of renewable aromatic compounds by catalytic fast pyrolysis of lignocellulosic biomass with bifunctional Ga/ZSM-5 catalysts. Angew. Chemie 124, 1416–1419.

Cui, H., Grace, J.R., 2008. Spouting of biomass particles: a review. Bioresour. Technol. 99, 4008–4020.

Dai, J., Cui, H., Grace, J.R., 2012. Biomass feeding for thermochemical reactors. Prog. Energy Combust. Sci. 38, 716–736.

Du, S., Valla, J.A., Bollas, G.M., 2013a. Characteristics and origin of char and coke from fast and slow, catalytic and thermal pyrolysis of biomass and relevant model compounds. Green Chem. 15, 3214–3229.

Du, Z., Hu, B., Ma, X., Cheng, Y., Liu, Y., Lin, X., Wan, Y., Lei, H., Chen, P., Ruan, R., 2013b. Catalytic pyrolysis of microalgae and their three major components: carbohydrates, proteins, and lipids. Bioresour. Technol. 130, 777–782.

Elordi, G., Olazar, M., Lopez, G., Castaño, P., Bilbao, J., 2011. Role of pore structure in the deactivation of zeolites (HZSM-5, Hβ and HY) by coke in the pyrolysis of polyethylene in a conical spouted bed reactor. Appl. Catal. B Environ. 102, 224–231.

Foster, A.J., Jae, J., Cheng, Y.-T., Huber, G.W., Lobo, R.F., 2012. Optimizing the aromatic yield and distribution from catalytic fast pyrolysis of biomass over ZSM-5. Appl. Catal. A Gen. 423–424, 154–161.

Huber, G.W., Iborra, S., Corma, A., 2006. Synthesis of transportation fuels from biomass: chemistry, catalysts, and engineering. Chem. Rev. 106, 4044–4098.

Iliopoulou, E.F., Stefanidis, S.D., Kalogiannis, K.G., Delimitis, A., Lappas, A.A., Triantafyllidis, K.S., 2012. Catalytic upgrading of biomass pyrolysis vapors using transition metal-modified ZSM-5 zeolite. Appl. Catal. B Environ. 127, 281–290.

Jae, J., Coolman, R., Mountziaris, T.J., Huber, G.W., 2014. Catalytic fast pyrolysis of lignocellulosic biomass in a process development unit with continual catalyst addition and removal. Chem. Eng. Sci. 108, 33–46.

Lappas, A.A., Samolada, M.C., Iatridis, D.K., Voutetakis, S.S., Vasalos, I.A., 2002. Biomass pyrolysis in a circulating fluid bed reactor for the production of fuels and chemicals. Fuel 81, 2087–2095.

Mante, O.D., Agblevor, F.a., Oyama, S.T., McClung, R., 2014. Catalytic pyrolysis with ZSM-5 based additive as co-catalyst to Y-zeolite in two reactor configurations. Fuel 117, 649–659.

Naqvi, S.R., Uemura, Y., Yusupa, S.B., 2014. Catalytic pyrolysis of paddy husk in a drop type pyrolyzer for bio-oil production: the role of temperature and catalyst. J. Anal. Appl. Pyrolysis 106, 57–62.

Nowakowski, D.J., Bridgwater, a.V., Elliott, D.C., Meier, D., de Wild, P., 2010. Lignin fast pyrolysis: results from an international collaboration. J. Anal. Appl. Pyrolysis 88, 53–72.

Olazar, M., Aguado, R., Bilbao, J., Barona, A., 2000. Pyrolysis of sawdust in a conical spouted-bed reactor with a HZSM-5 catalyst. AIChE J. 46, 1025–1033.

Park, H.J., Park, K.-H., Jeon, J.-K., Kim, J., Ryoo, R., Jeong, K.-E., Park, S.H., Park, Y.-K., 2012. Production of phenolics and aromatics by pyrolysis of miscanthus. Fuel 97, 379–384.

Patwardhan, P.R., Dalluge, D.L., Shanks, B.H., Brown, R.C., 2011. Distinguishing primary and secondary reactions of cellulose pyrolysis. Bioresour. Technol. 102, 5265–5269.

Pütün, E., Uzun, B.B., Pütün, A.E., 2006. Fixed-bed catalytic pyrolysis of cotton-seed cake: effects of pyrolysis temperature, natural zeolite content and sweeping gas flow rate. Bioresour. Technol. 97, 701–710.

Srinivasan, V., Adhikari, S., Chattanathan, S.A., Park, S., 2012. Catalytic Pyrolysis of Torrefied Biomass for Hydrocarbons Production.

Stefanidis, S.D., Kalogiannis, K.G., Iliopoulou, E.F., Lappas, A.A., Pilavachi, P.A., 2011. In-situ upgrading of biomass pyrolysis vapors: catalyst screening on a fixed bed reactor. Bioresour. Technol. 102, 8261–8267.

Thangalazhy-Gopakumar, S., Adhikari, S., Chattanathan, S.A., Gupta, R.B., 2012. Catalytic pyrolysis of green algae for hydrocarbon production using H^+ZSM-5 catalyst. Bioresour. Technol. 118, 150–157.

Wang, K., Brown, R.C., 2013. Catalytic pyrolysis of microalgae for production of aromatics and ammonia. Green Chem. 15, 675–681.

Wang, K., Kim, K.H., Brown, R.C., 2014. Catalytic pyrolysis of individual components of lignocellulosic biomass. Green Chem. 16, 727–735.

Wang, L., Lei, H., Ren, S., Bu, Q., Liang, J., Wei, Y., Liu, Y., Lee, G.-S.J., Chen, S., Tang, J., Zhang, Q., Ruan, R., 2012. Aromatics and phenols from catalytic pyrolysis of Douglas fir pellets in microwave with ZSM-5 as a catalyst. J. Anal. Appl. Pyrolysis 98, 194–200.

Williams, P.T., Nugranad, N., 2000. Comparison of products from the pyrolysis and catalytic pyrolysis of rice husks. Energy 25, 493–513.

Yu, Y., Li, X., Su, L., Zhang, Y., Wang, Y., Zhang, H., 2012. The role of shape selectivity in catalytic fast pyrolysis of lignin with zeolite catalysts. Appl. Catal. A Gen. 447–448, 115–123.

Zhang, H., Carlson, T.R., Xiao, R., Huber, G.W., 2012. Catalytic fast pyrolysis of wood and alcohol mixtures in a fluidized bed reactor. Green Chem. 14, 98–110.

Zhang, H., Xiao, R., Huang, H., Xiao, G., 2009. Comparison of non-catalytic and catalytic fast pyrolysis of corncob in a fluidized bed reactor. Bioresour. Technol. 100, 1428–1434.

Zheng, A., Zhao, Z., Chang, S., Huang, Z., Wu, H., Wang, X., He, F., Li, H., 2014. Effect of crystal size of ZSM-5 on the aromatic yield and selectivity from catalytic fast pyrolysis of biomass. J. Mol. Catal. A Chem. 383–384, 23–30.